Introduction to Turbulence

OCN/MET 665

Transition to Turbulence

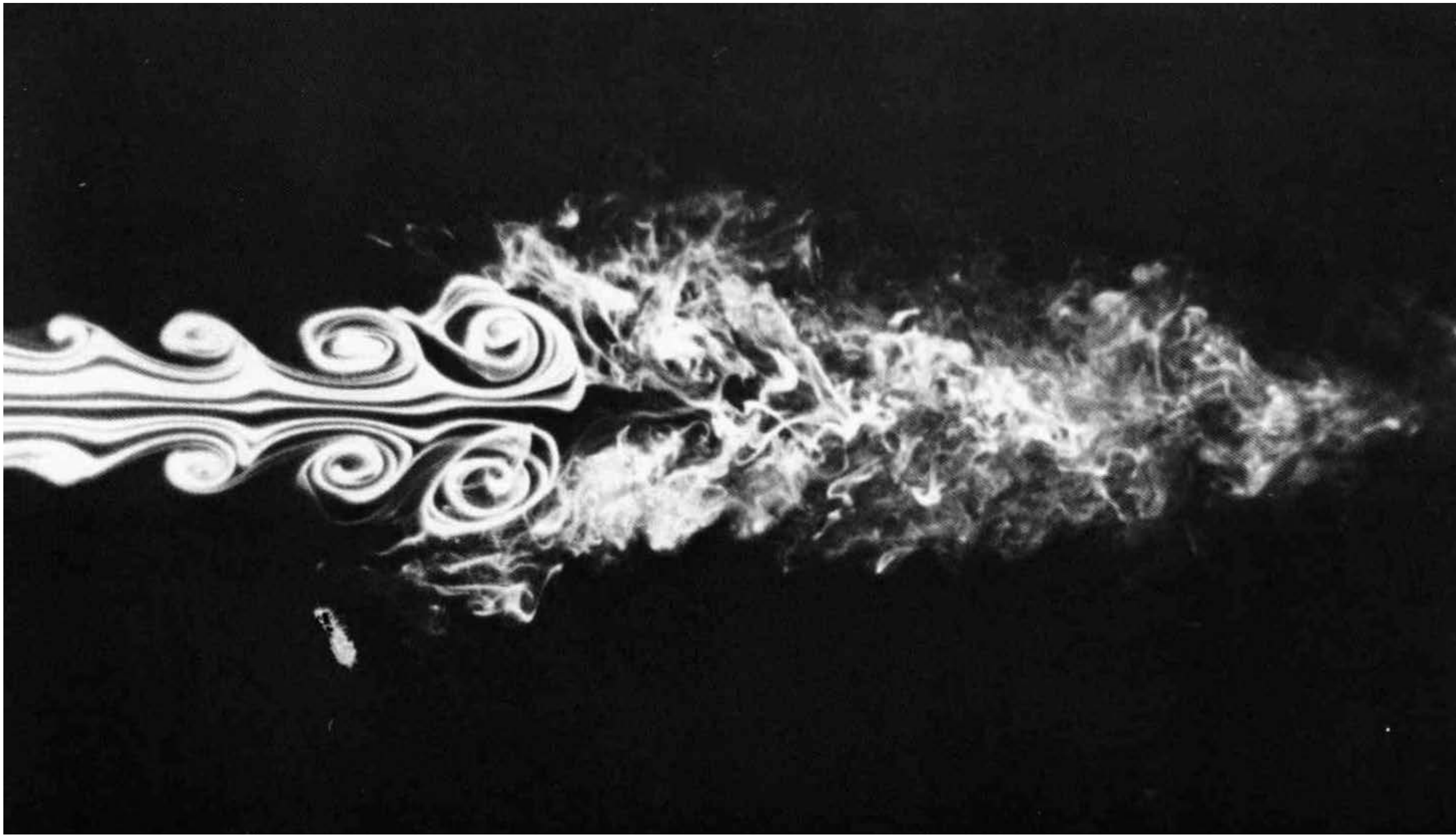

An album of fluid motion. Van Dyke

Osborne Reynolds 1883

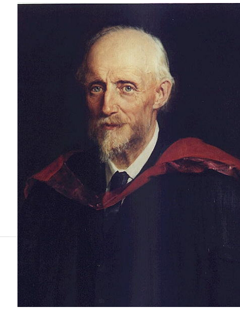

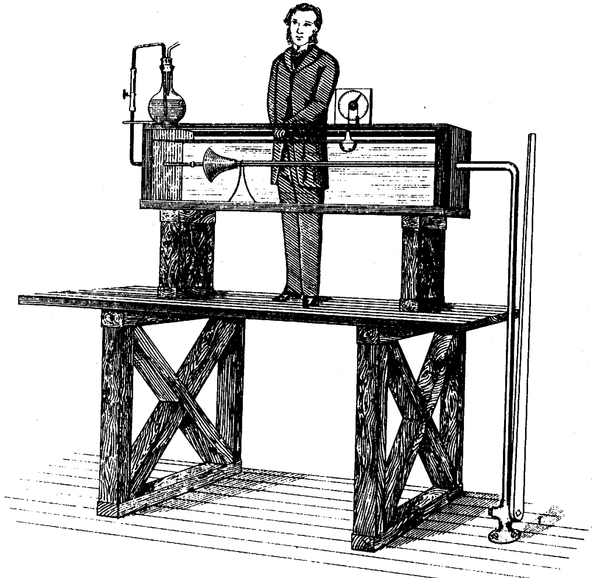

Fig. 9.1. Sketch of Reynolds's dye experiment, taken from his 1883 paper

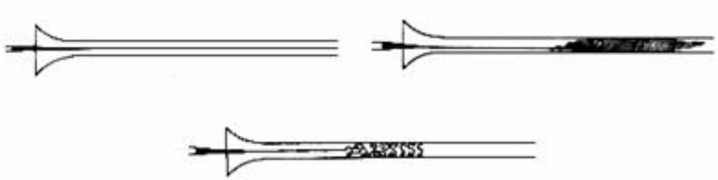

Reynolds' sketches of the transition from laminar to turbulent flow.

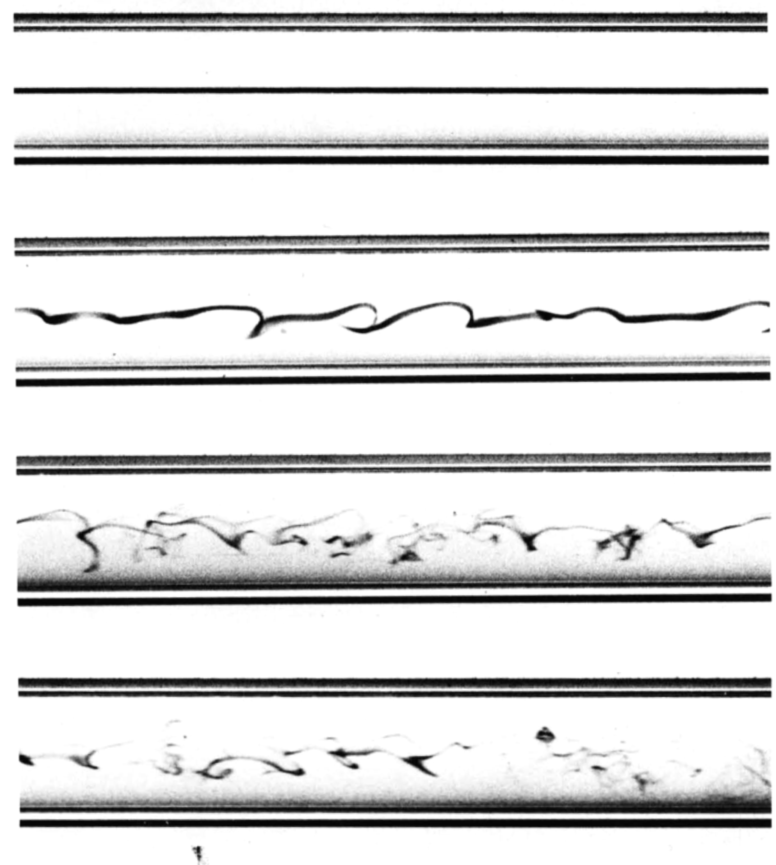

103. Repetition of Reynolds' dye experiment. Osborne Reynolds' celebrated 1883 investigation of stability of flow in a tube was documented by sketches rather than photography. However the original apparatus has survived at the University of Manchester. Using it a century later, N. H. Johannesen and C. Lowe have taken this sequence of photographs. In laminar flow a filament of colored water introduced at a bell-shaped entry extends undisturbed the whole length of the glass tube. Transition is seen in the second of the photographs as the speed is increased; and the last two photographs show fully turbulent flow. Modern traffic in the streets of Manchester made the critical Reynolds number lower than the value 13,000 found by Reynolds.

Shear Instability

Reynolds Number:

$$Re = \frac{UL}{\nu}$$

Critical Reynolds number

$Re \gtrsim O(1000)$

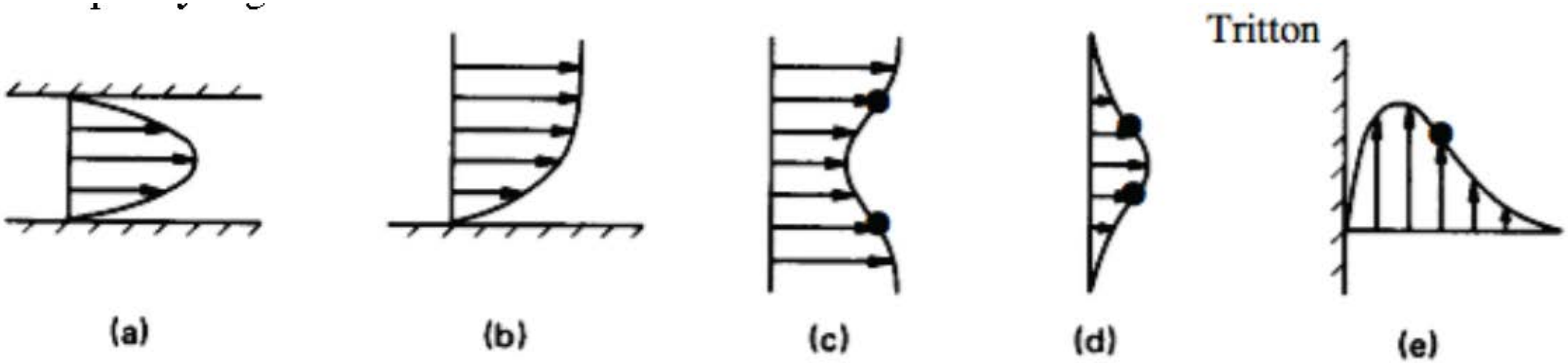

Figure 17.13 To illustrate that the velocity profiles of (a) pipe flow, (b) a boundary layer, (c) a wake, (d) a jet, and (e) a free convection boundary layer are all shear flows.

Some shear flows. Dots indicate inflection points.

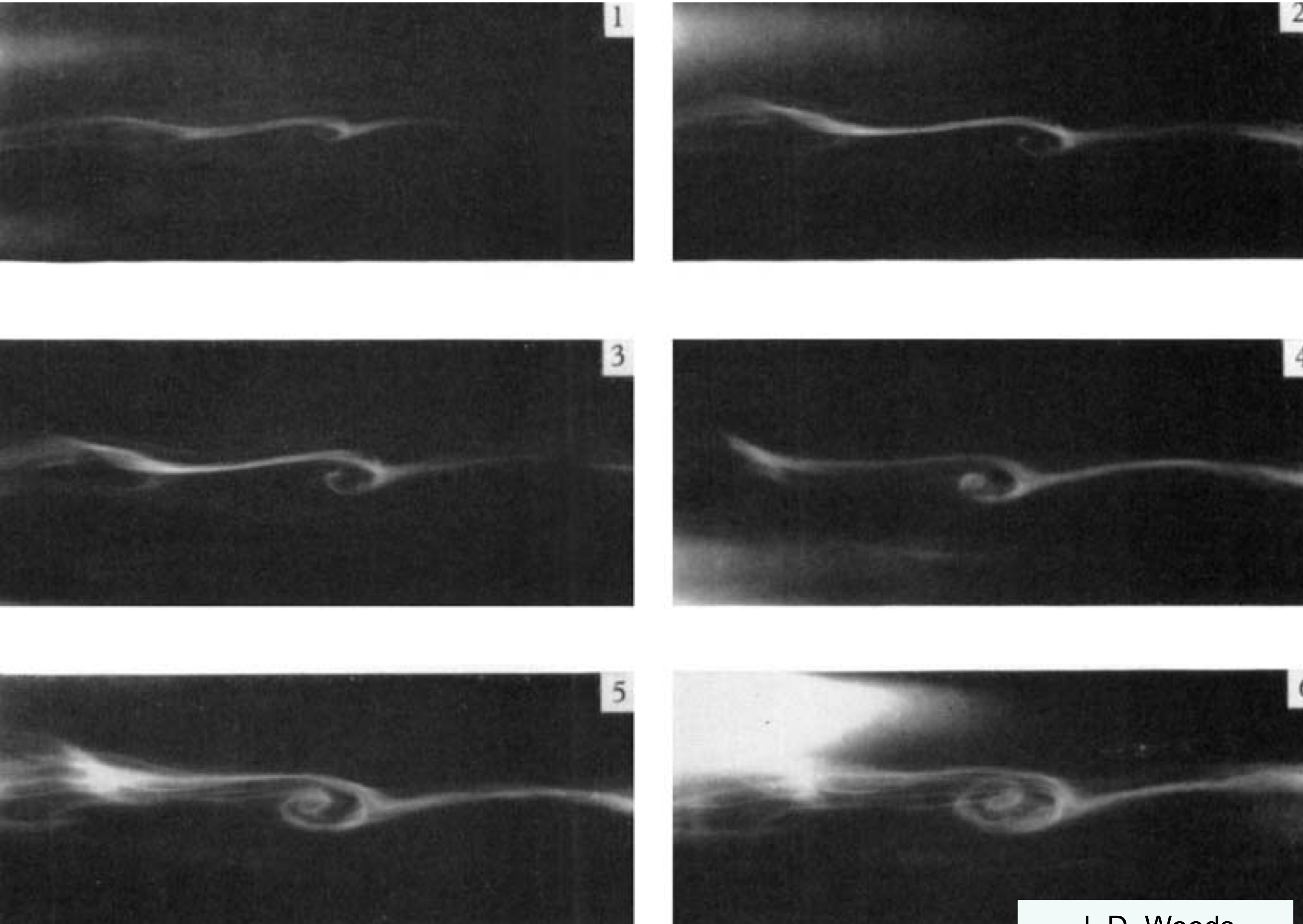

J. D. Woods
(1968)

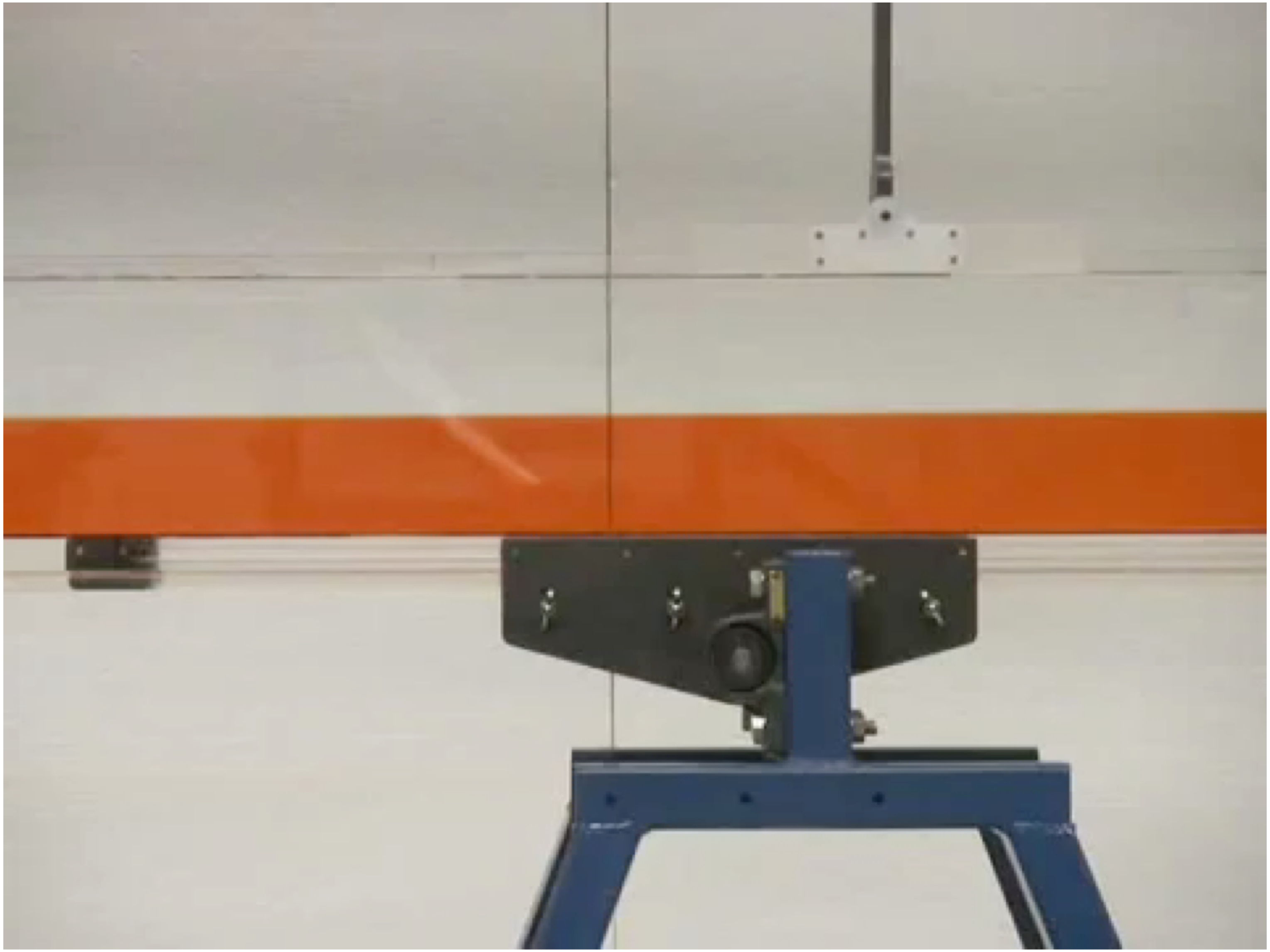

Grae Worcester, University of Cambridge

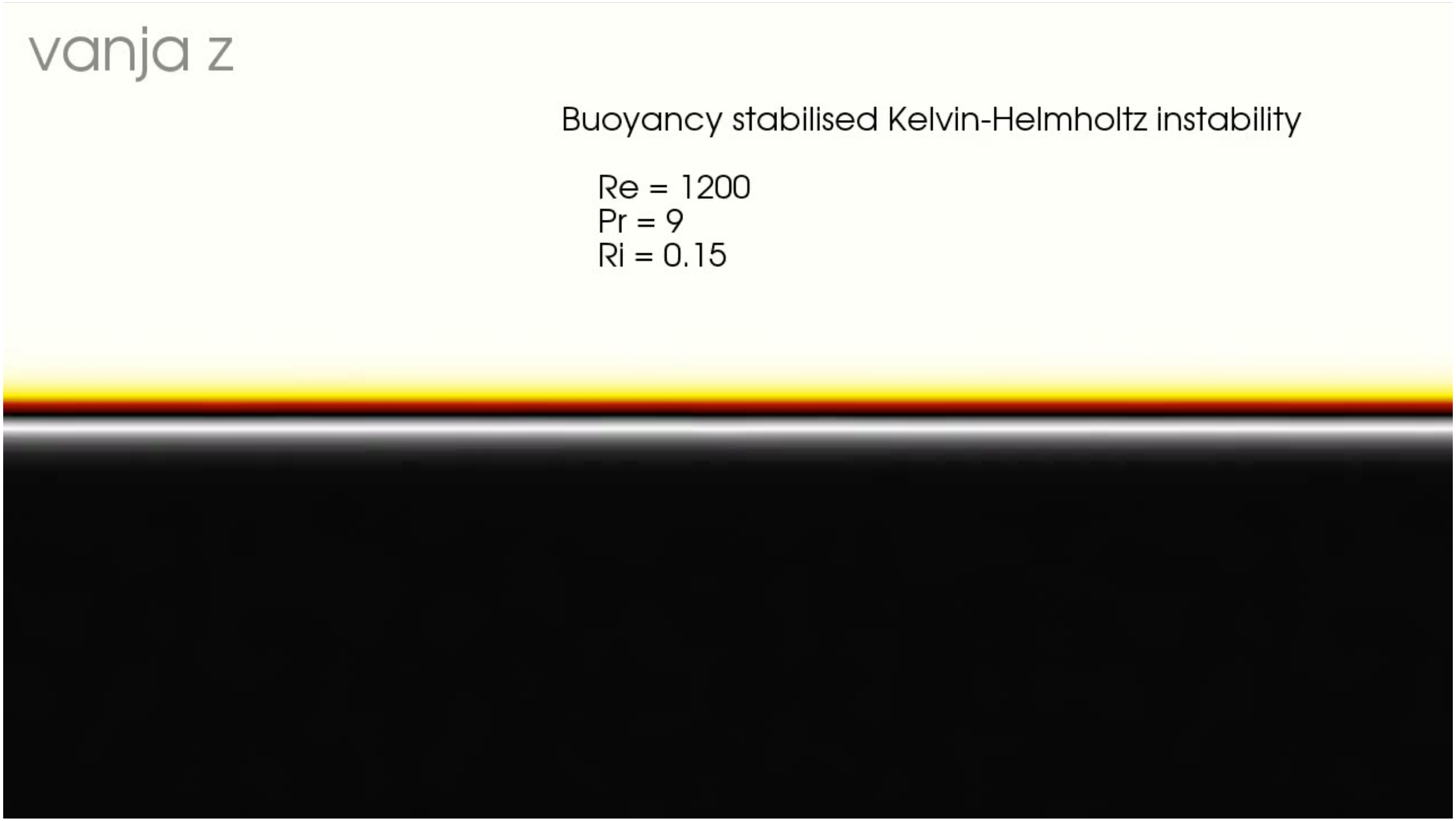

Vanja Zecevic, University of Sydney

Kelvin-Helmholtz Instability

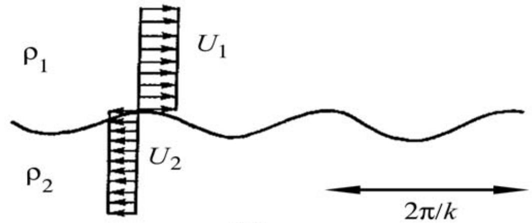

(a)

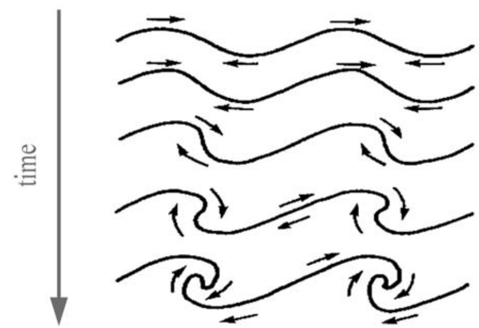

(b)

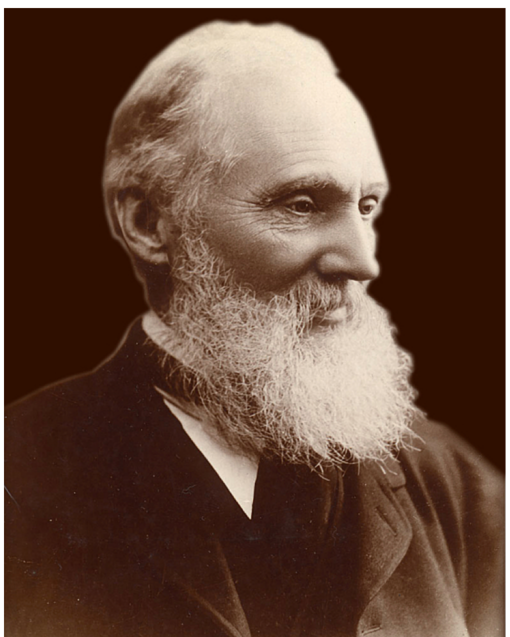

Helmholtz (1868)
Kelvin (1871)

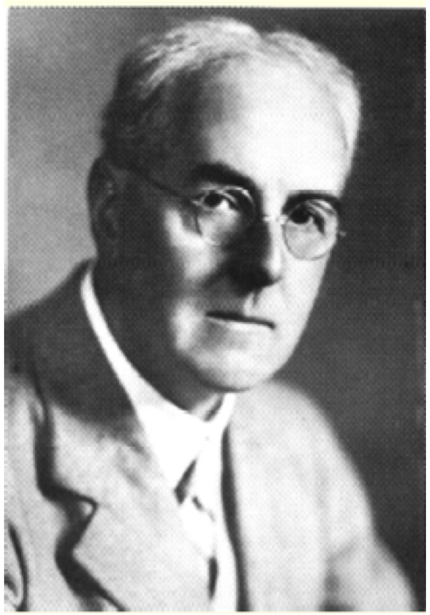

Lewis Fry Richardson

Richardson Number

Necessary condition for instability:

$$R_i \left(= \frac{N^2}{S^2} \right) \leq 0.25$$

somewhere in the flow
Miles (1961), Howard (1961)

$$N = \sqrt{-\frac{g}{\rho_o}\frac{\partial \rho(z)}{\partial z}}$$

Thorpe (1987, JGR 92, C5, 5231-5248

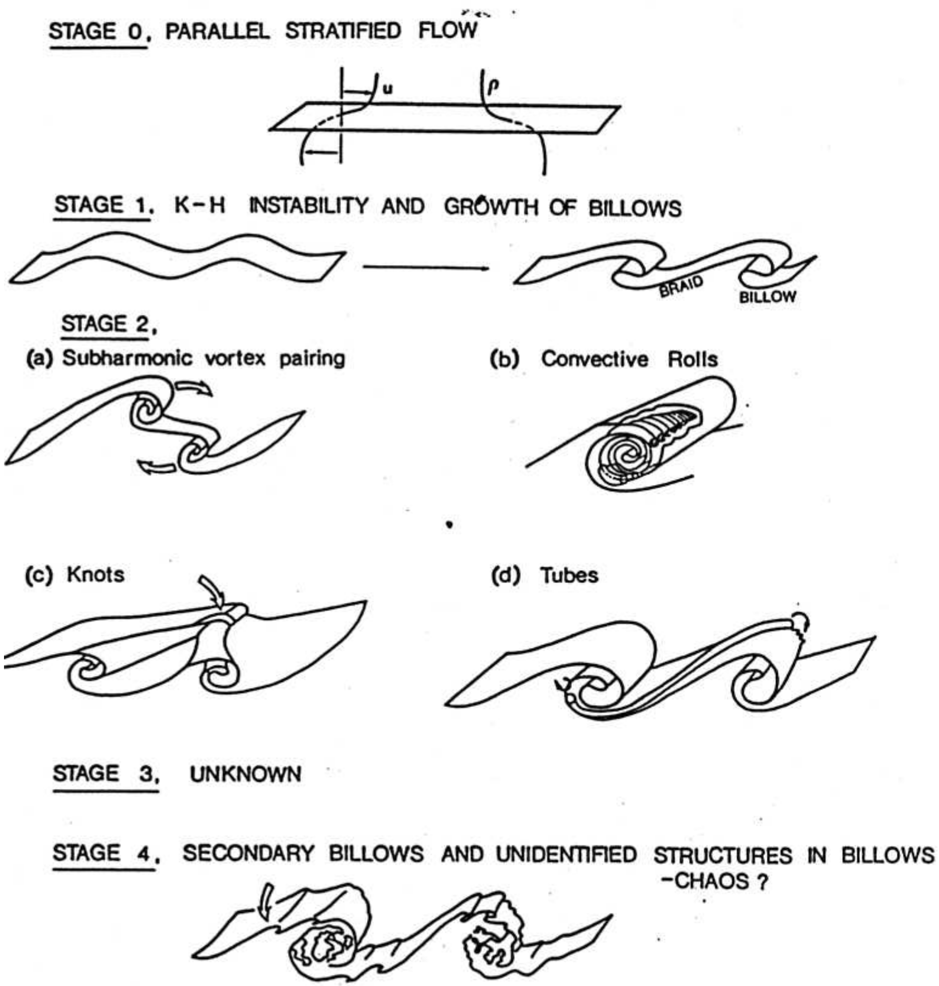

Fig. 7. Stages in the transition to turbulence of Kelvin-Helmholtz instability.

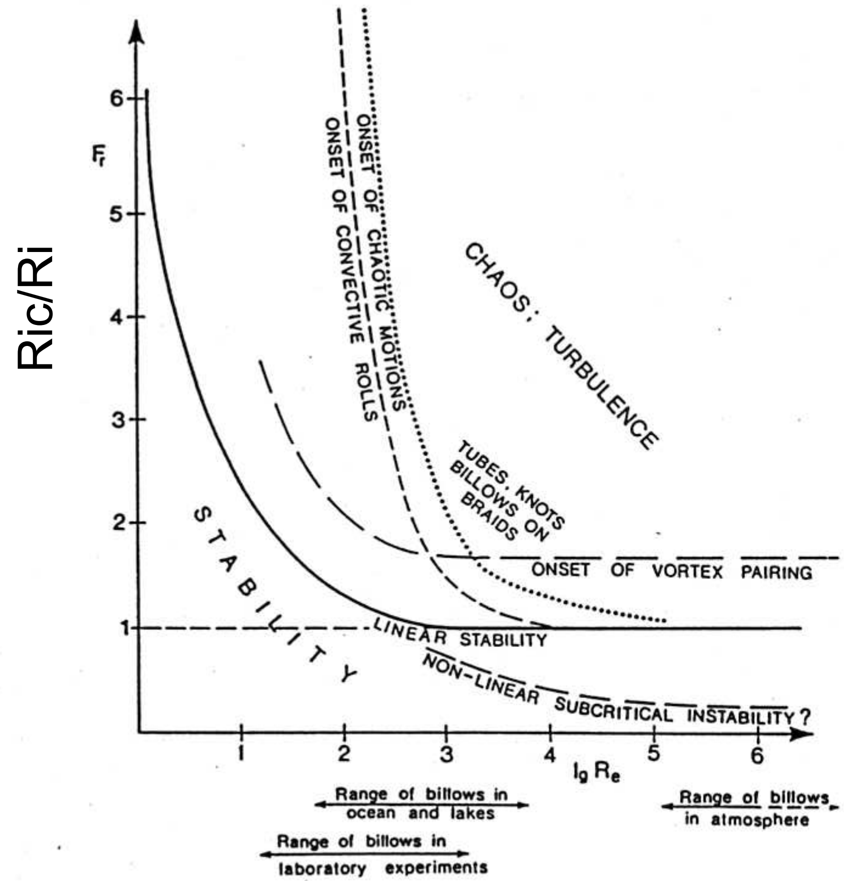

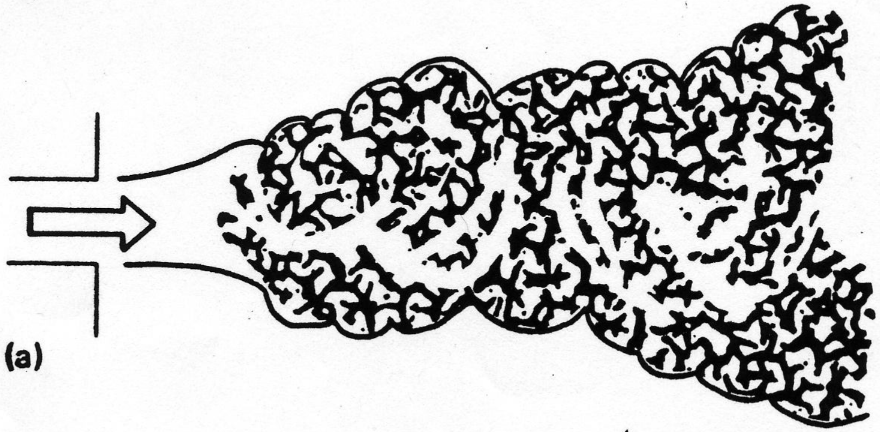

(a)

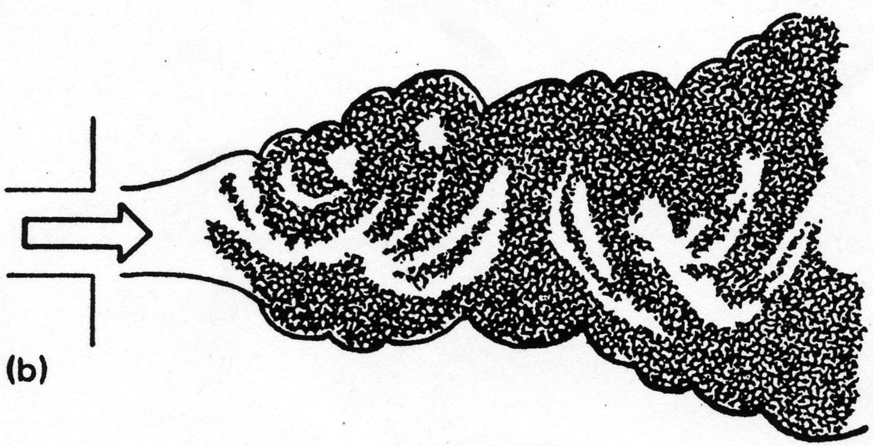

(b)

Figure 1.6. Turbulent jets at different Reynolds numbers: (a) relatively low Reynolds number, (b) relatively high Reynolds number (adapted from a film sequence by R. W. Stewart, 1969). The shading pattern used closely resembles the small-scale structure of turbulence seen in shadowgraph pictures.

Convection

Rayleigh Number:

$$Ra = \frac{g\alpha\Delta T d^3}{\nu\kappa}$$

ΔT temperature difference
d   distance between plates
α coef of expansion
ν kinematic viscosity
κ thermal diffusivity

Lord Rayleigh (John Strutt)
(1842-1919)

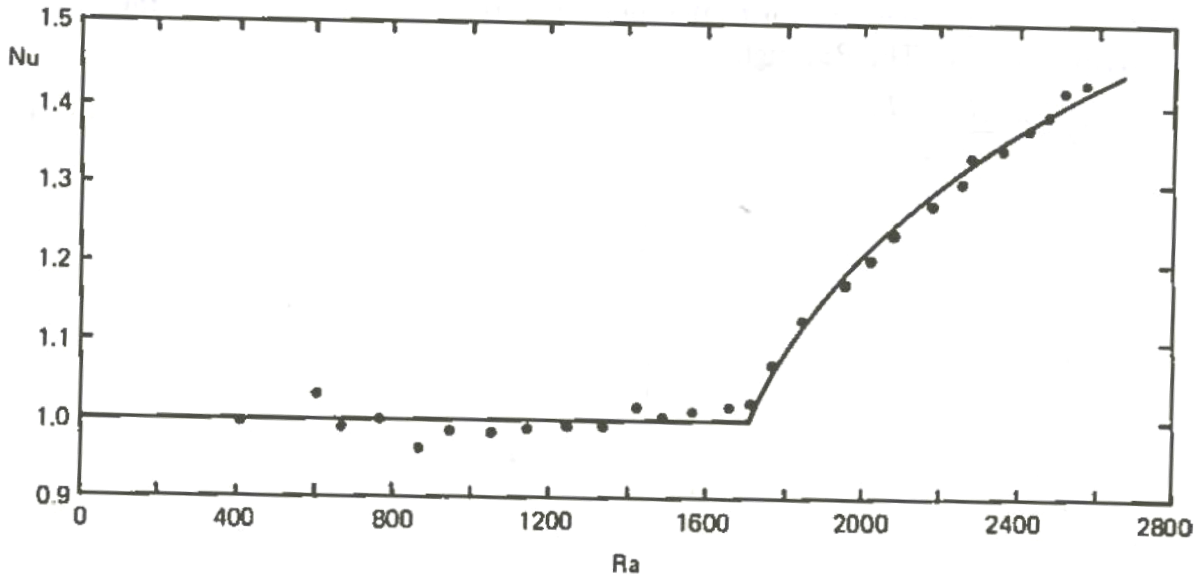

Figure 4.4 Variation of Nusselt number with Rayleigh number for Bénard convection, showing increase of heat transfer with onset of motion. Data obtained by C. W. Titman.

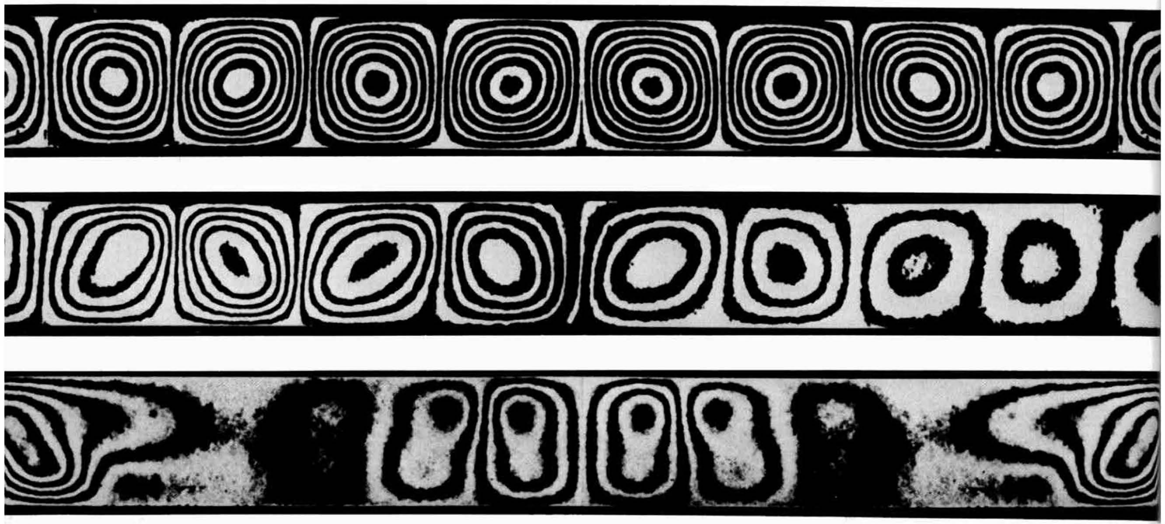

139. Buoyancy-driven convection rolls. Differential interferograms show side views of convective instability of silicone oil in a rectangular box of relative dimensions 10:4:1 heated from below. At the top is the classical Rayleigh-Bénard situation: uniform heating produces rolls parallel to the shorter side. In the middle photograph the temperature difference and hence the amplitude of motion increase from right to left. At the bottom, the box is rotating about a vertical axis. *Oertel & Kirchartz 1979, Oertel 1982*a

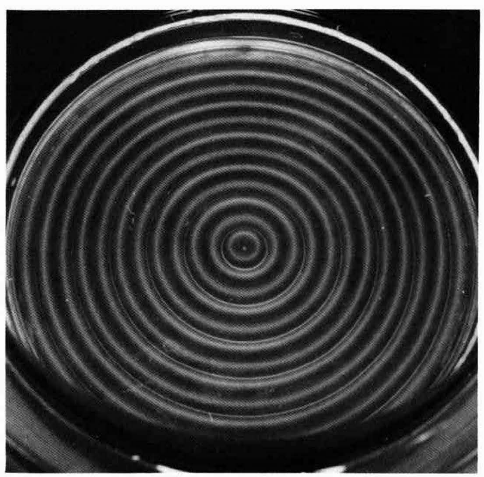

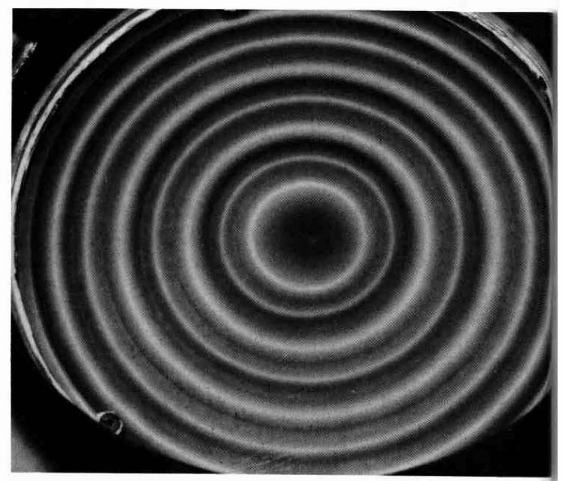

140. Circular buoyancy-driven convection cells. Silicone oil containing aluminum powder is covered by a uniformly cooled glass plate, which eliminates surface-tension effects. The circular boundary induces circular rolls. In the left photograph the copper bottom is uniformly heated at 2.9 times the critical Rayleigh number, giving regular rolls. At the right, the bottom is hotter at the rim than at the center. This induces an overall circulation which, superimposed on regular circular rolls, produces alternately larger and smaller rolls. *Koschmieder 1974, 1966*

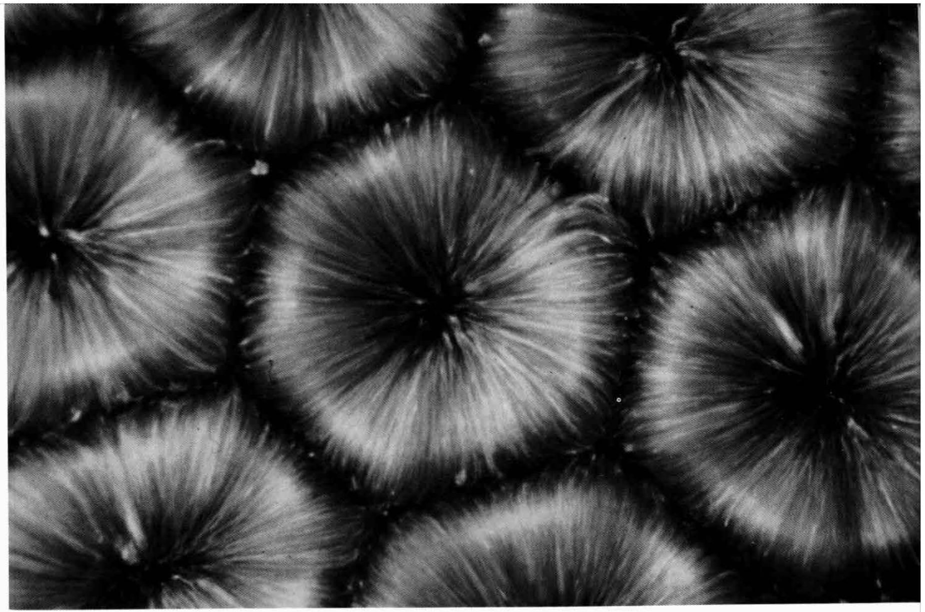

141. Surface-tension-driven (Bénard) convection. A top view, magnified some 25 times, shows the hexagonal convection pattern in a layer of silicone oil 1 mm deep that is heated uniformly below and exposed to ambient air above. With the upper surface free, the flow is driven mainly by inhomogeneities in surface tension, rather than by buoyancy as on the previous page. Light reflected from aluminum flakes shows fluid rising at the center of each cell and descending at the edges. The exposure time is 10 s, whereas fluid moves across the cell from the center to the edge in 2 s. *Photograph by* M. G. *Velarde,* M. *Yuste, and* J. *Salan*

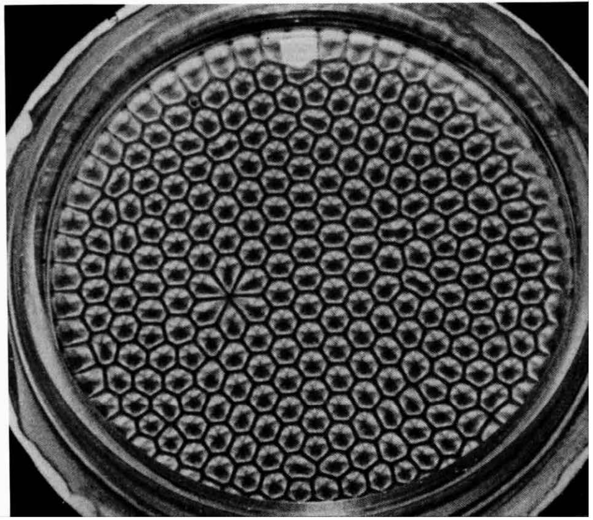

142. Imperfections in a hexagonal Bénard convection pattern. The hexagonal pattern of cells typical of convective instability driven primarily by surface tension is seen to accommodate itself to a circular boundary. Aluminum powder shows the flow in a thin layer of silicone oil of kinematic viscosity 0.5 cm^2/s on a uniformly heated copper plate. A tiny dent in the plate causes the imperfection at the left, forming diamond-shaped cells. This shows how sensitive the pattern is to small irregularities. *Koschmieder 1974*

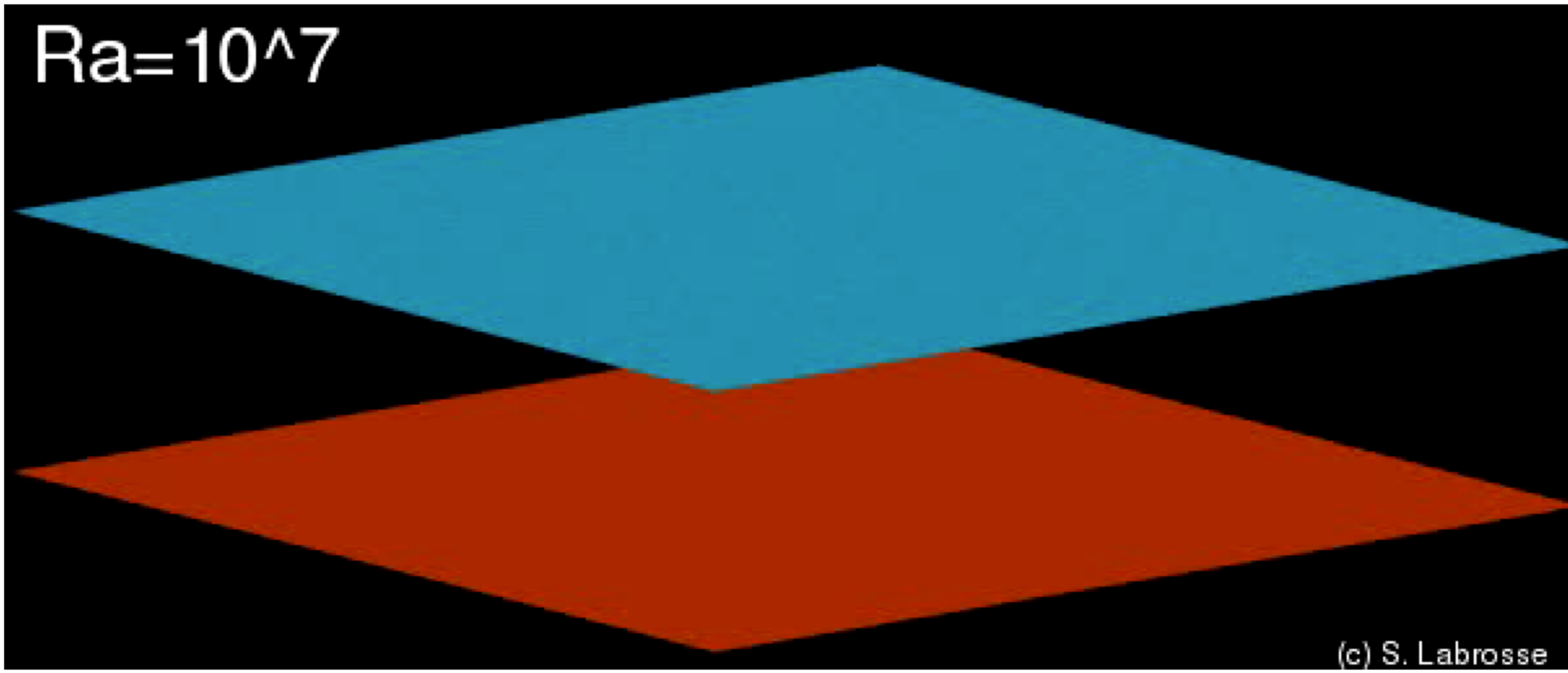
Ra=10^7
(c) S. Labrosse

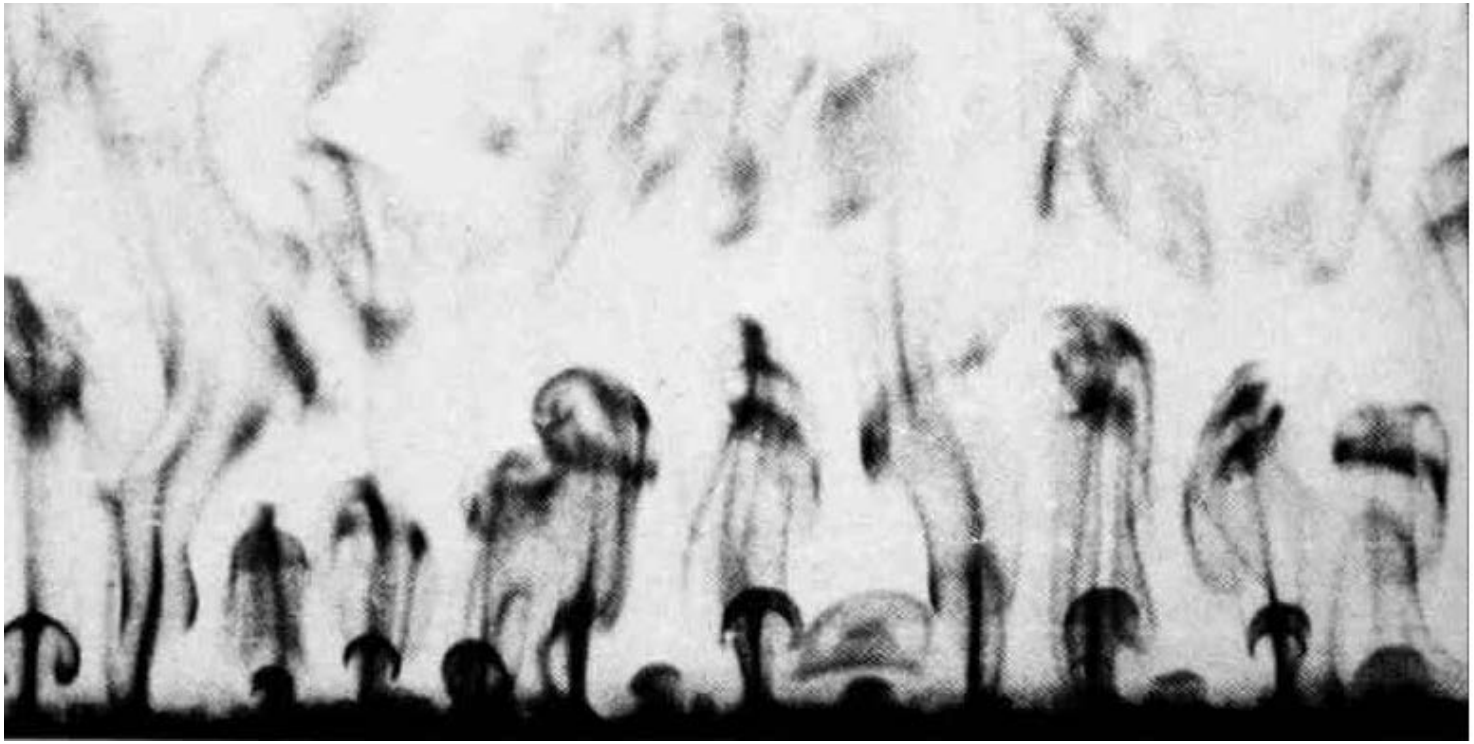

Turbulence characteristics

- 3-dimensional
- rotational $\nabla \times \vec{V} \neq 0$
  – carries vorticity (unlike linear surface waves)
- irregular, unpredictable (random) motion – described by probability density function
- diffusive – several orders of magnitude greater than molecular diffusion
- dissipative – K.E.$\rightarrow$ heat
  requires steady supply of energy

Turbulence characteristics

- flow has large Reynolds #, $\mathrm{Re} = \frac{Ul}{\nu} \geq 10^3$ (nonlinear)
- does not obey a dispersion relation (not wavelike)
- broad wavenumber spectrum
- generally anisotropic at larger scales
- is a function of the flow, not the fluid
- satisfies Navier-Stokes equations

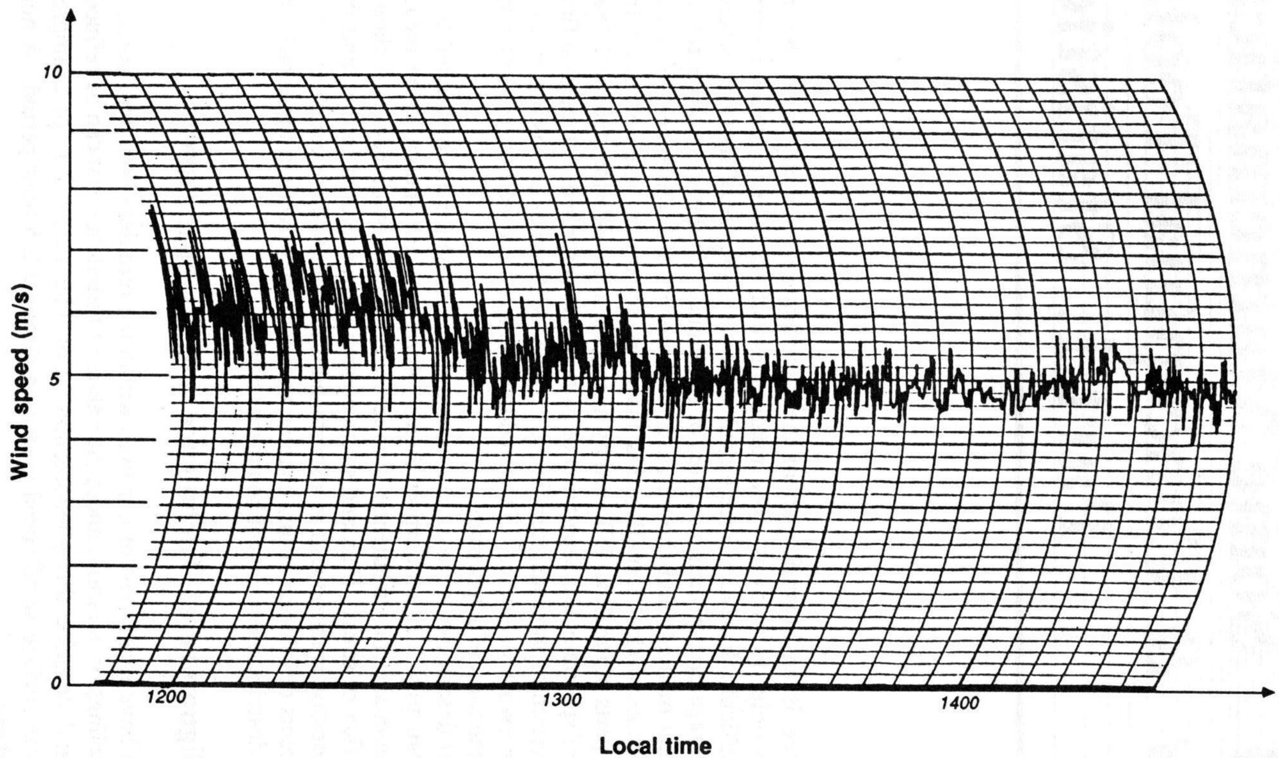

Fig. 2.1 Trace of wind speed obseved in early afternoon.

Fig. 1.3
Idealization of (a) Mean wind alone, (b) waves alone, and (c) turbulence alone. In reality waves or turbulence are often superimposed on a mean wind. U is the component of wind in the x-direction.

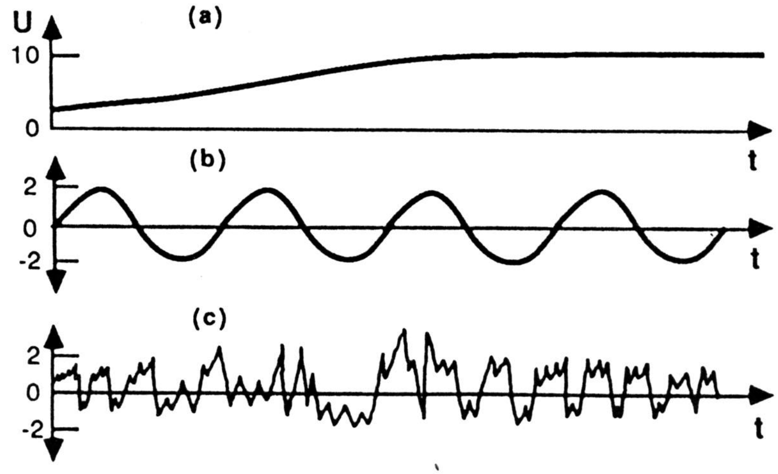

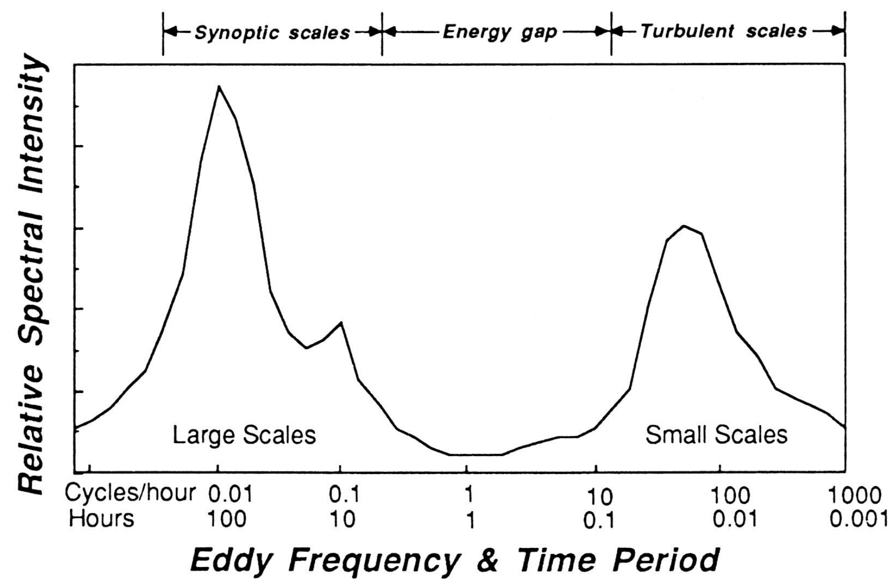

Fig. 2.2 Schematic spectrum of wind speed near the ground estimated from a study of Van der Hoven (1957).

Stirring and Mixing

- Stirring increases area of contact
- Sharpens gradients and reduces scales down to those where molecular diffusivity acts
- Molecular diffusivity results in irreversible mixing

adapted from Eckart (1948)

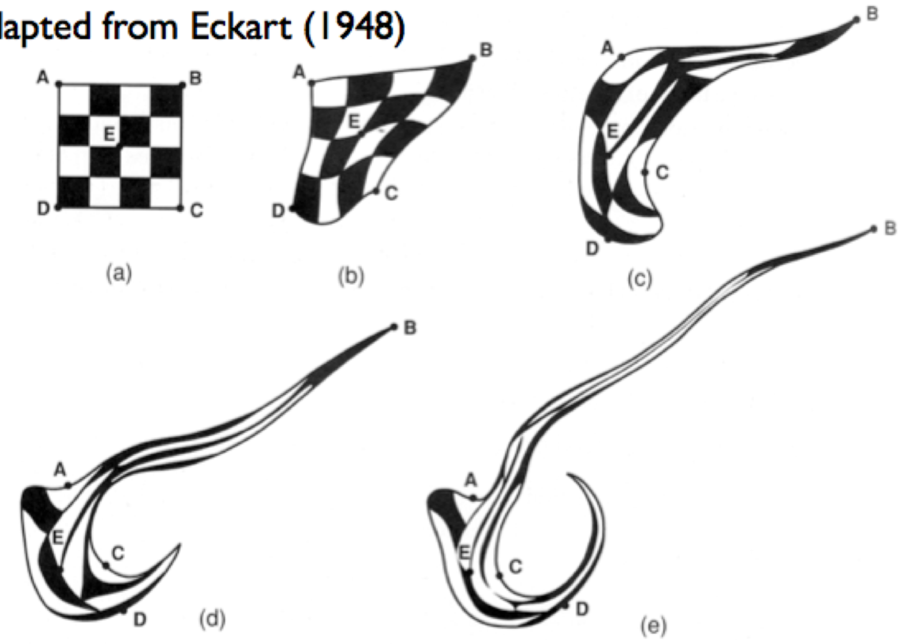

Mixing in turbulent flow ≫ Mixing in laminar flow

Diffusion alone

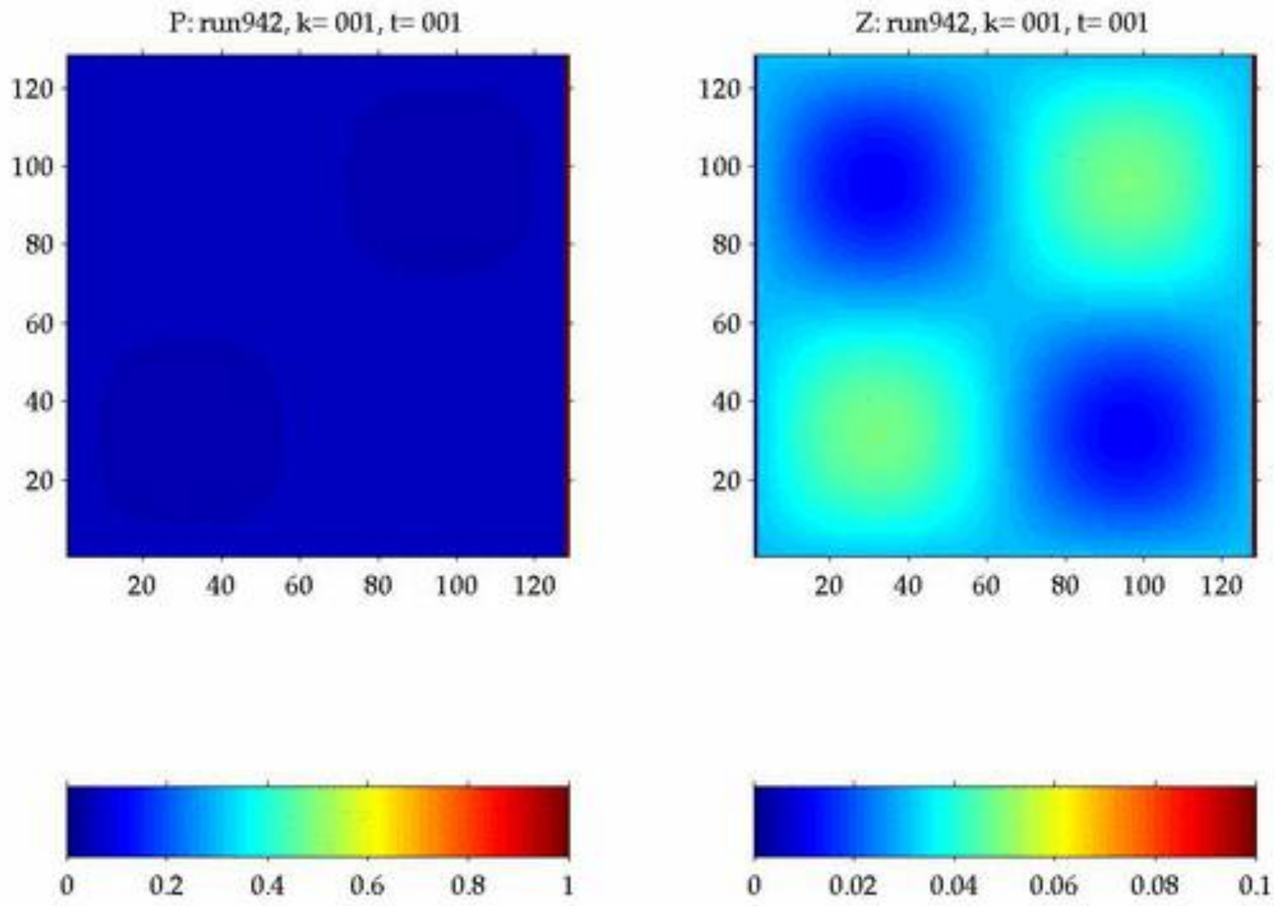

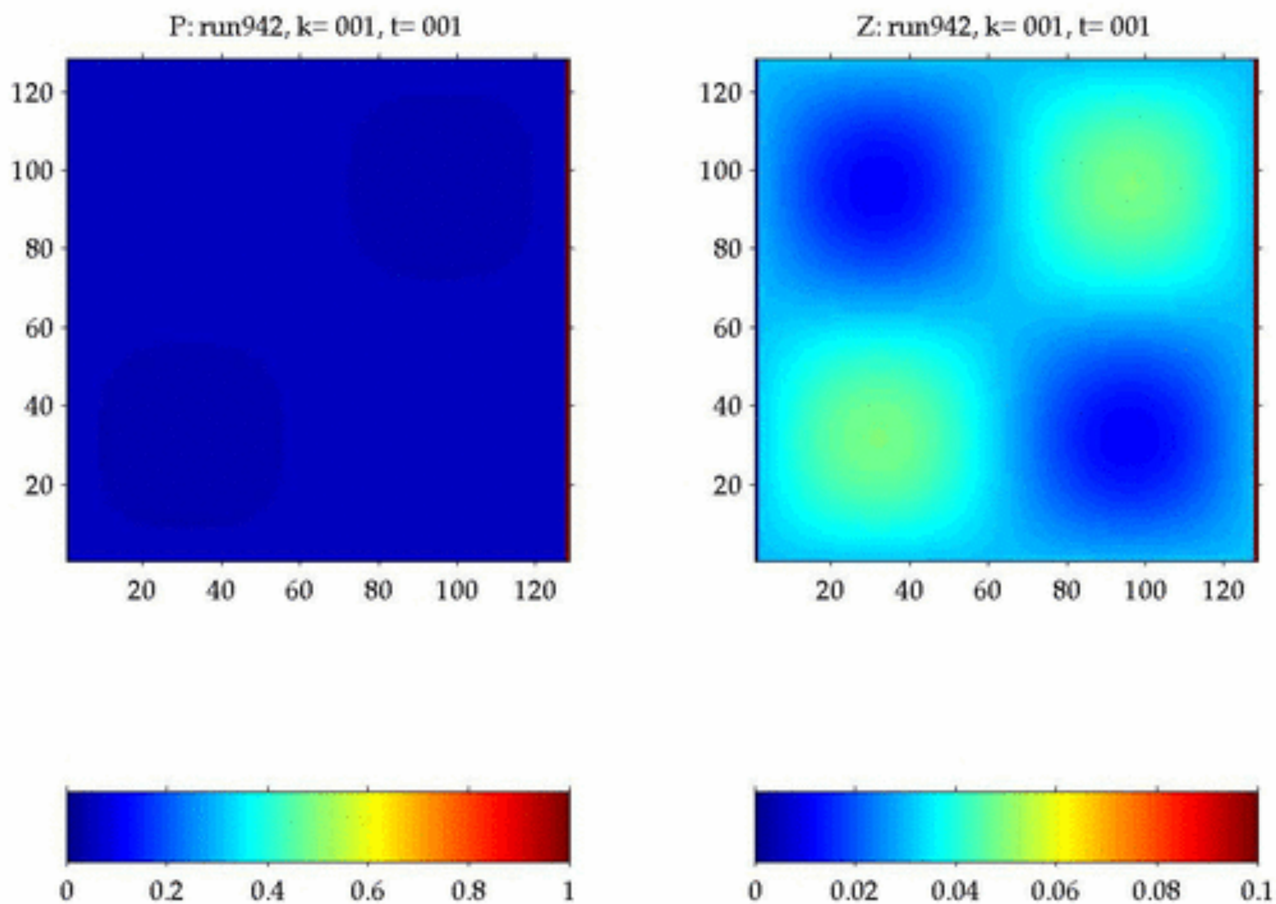
P: run942, k= 001, t= 001
Z: run942, k= 001, t= 001
120
100
80
60
40
20
20 40 60 80 100 120
0 0.2 0.4 0.6 0.8 1
0 0.02 0.04 0.06 0.08 0.1

Stirring

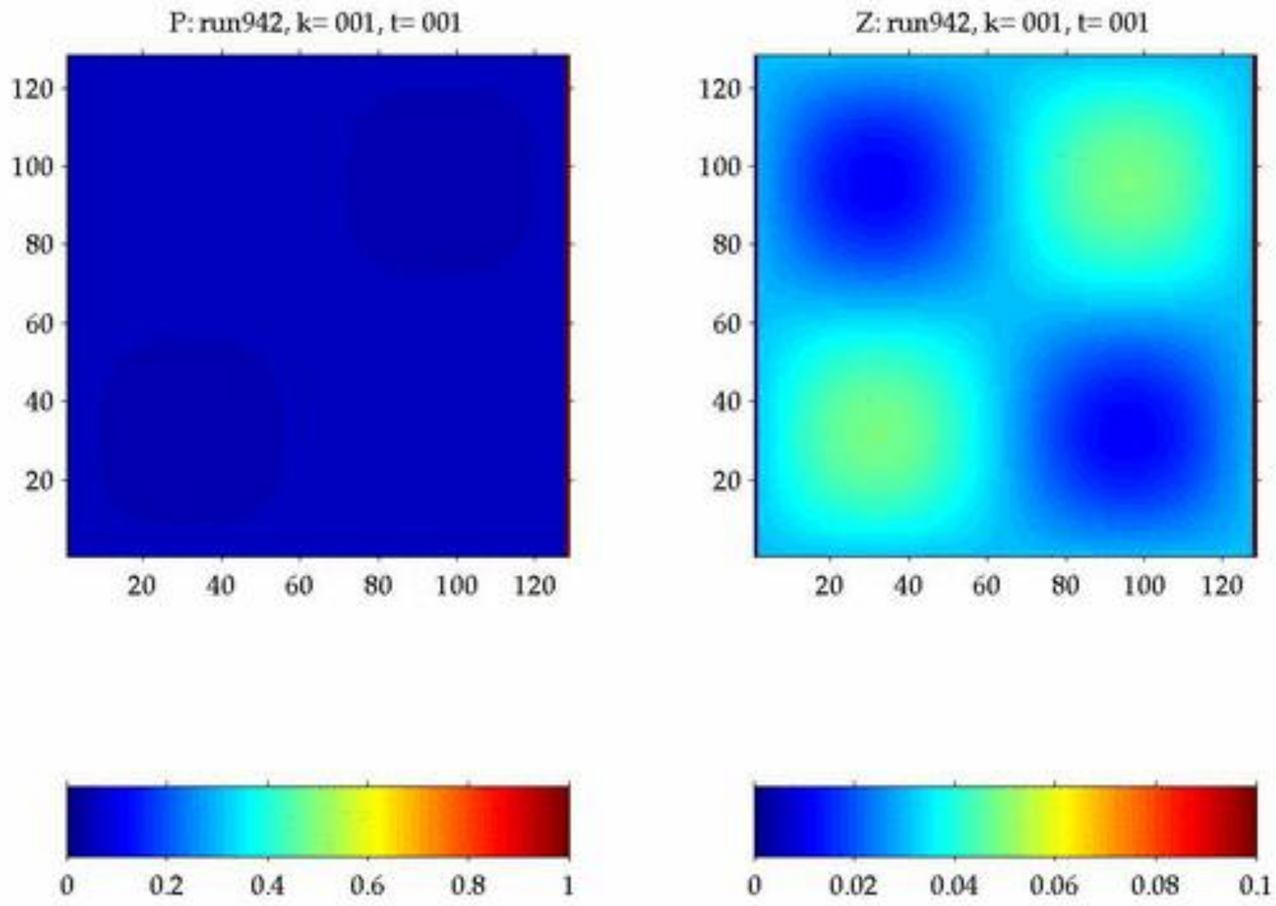

P: run942, k= 001, t= 001
Z: run942, k= 001, t= 001
120
100
80
60
40
20
20 40 60 80 100 120
0 0.2 0.4 0.6 0.8 1
0 0.02 0.04 0.06 0.08 0.1

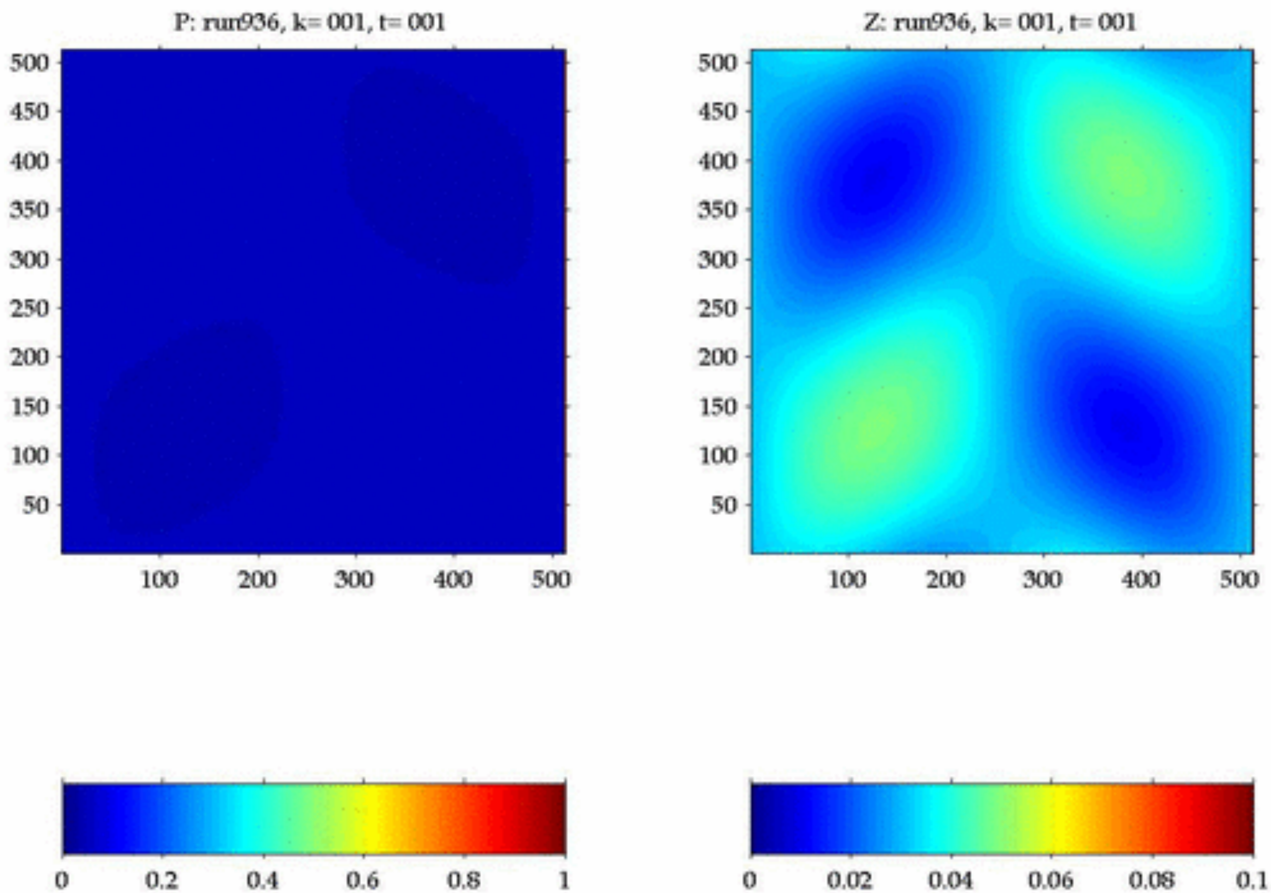
P: run936, k= 001, t= 001
Z: run936, k= 001, t= 001
500
450
400
350
300
250
200
150
100
50
100
200
300
400
500
0
0.2
0.4
0.6
0.8
1
0
0.02
0.04
0.06
0.08
0.1

Energy Cascade (Kolmogorov ,1941)

Figure 8.3 Schema of energy spectrum in three-dimensional turbulence, in the theory of Kolmogorov. Energy is supplied at some rate ε; it is transferred ('cascaded') to small scales, where it is ultimately dissipated by viscosity. There is no systematic energy transfer to scales larger than the forcing scale, so here the energy falls off.

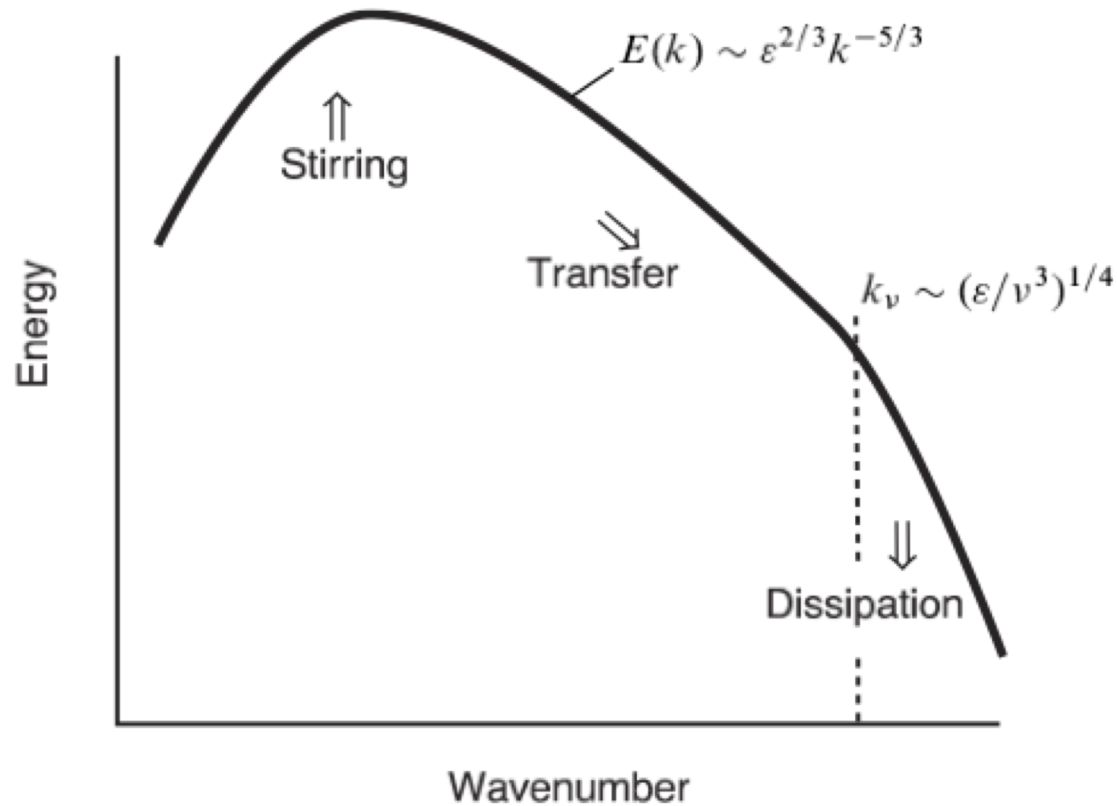

If $\mathcal{E} = f(\varepsilon, k)$ then the only dimensionally consistent relation for the energy spectrum is

$$\mathcal{E} = \mathcal{K} \varepsilon^{2/3} k^{-5/3}$$

Energy Cascade (L. F. Richardson ,1922)

"Big whirls have little whirls
that feed on their velocity,
and little whirls have smaller whirls
and so on to viscosity"

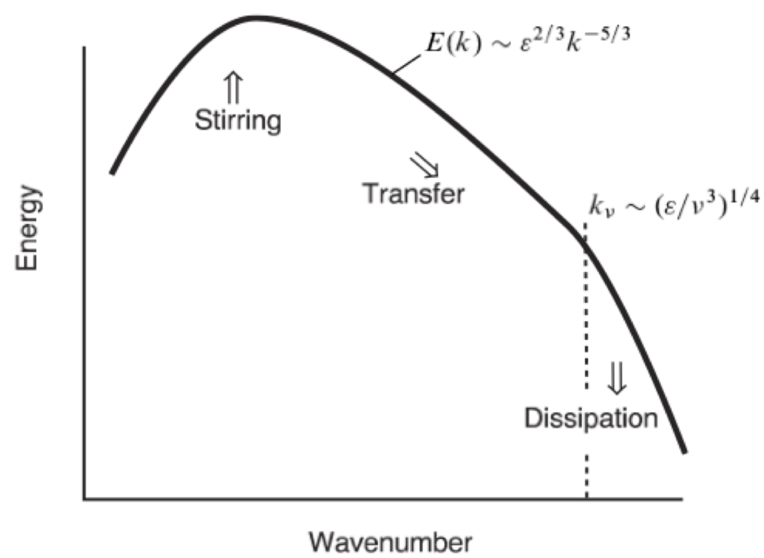

TURBULENT MIXING

• **MIXING**: Irreversible destruction of scalar and velocity gradients through the action of molecular diffusivities κ and viscosity ν

In a turbulent fluid, scalar and velocity gradients exist down to Batchelor and Kolmogorov scales:

For Ocean

$$L_b \sim 2\pi\left(\kappa^2 \upsilon / \varepsilon\right)^{1/4}$$

$$L_k \sim 2\pi\left(\upsilon^3 / \varepsilon\right)^{1/4}$$

Momentum $\nu = 1 \times 10^{-6} m^2 s^{-1}$

Thermal $\kappa_T = 1.4 \times 10^{-7} m^2 s^{-1}$

Salt $\kappa_S = 1 \times 10^{-9} m^2 s^{-1}$

Typical deep ocean TKE dissipation rate $\varepsilon \sim 10^{-9}$ W kg^{-1}
(1 hair dryer/km^3)

$\Rightarrow L_b$ & L_k ~ millimeters to centimeters

TURBULENT MIXING OCCURS AT SMALL SCALES

Homework:

Compare the Batchelor and Kolmogorov length scales in the deep and surface ocean where the dissipation rate is typically $\varepsilon=10^{-9}$ and 10^{-5} W kg^{-1}, respectively.

What are the scales in the atmospheric boundary layer under different conditions?

Vertical turbulent transports

- What is a turbulent flux?
  - **Reynolds' decomposition:** <wT> = <w><T> + <w'T'>
- What determines the vertical distribution of turbulence?
  - **TKE equation:** dTKE/dt = production – dissipation + advection
- How does turbulence determine the interfacial fluxes of heat, moisture and momentum?
  - Near-surface gradients and TKE levels are related.
- How are vertical turbulent transports modeled?
  - Flux profile relationships (Monin-Obukhov similarity theory)
  - closure schemes (parameterizations)
  - layered versus level models

Turbulent Flux Definitions

$$Sensible\,Heat : H_s = \rho_a c_{pa} \overline{w'T'}$$

$$Latent\,Heat : H_l = \rho_a L_e \overline{w'q'}$$

$$Stress : \vec{\tau} = \rho_a \overline{w'u_x'}\,\hat{i} + \rho_a \overline{w'u_y'}\,\hat{j}$$